Near-threshold behavior of the cross sections of $\gamma p \to \phi p$ and $\gamma d \to \phi pn$: A resonance interpretation

JLAB and Indiana University

January 18, 2013

Alvin Stanza Kiswandhi[1]

In collaboration with:
Shin Nan Yang[1], **Yu Bing Dong**[2], **and Ju-Jun Xie**[1]

1 Center for Theoretical Sciences and Department of Physics, National Taiwan University, Taipei 10617, Taiwan
2 Institute of High Energy Physics, Chinese Academy of Sciences, Beijing 100049, China

Motivation

- Presence of **a local peak near threshold** at $E_\gamma \sim 2.0$ GeV in the **differential cross-section (DCS) of $\gamma p \to \phi p$ at forward angle** by **Mibe and Chang, et al.** [PRL **95** 182001 (2005)] from the LEPS Collaboration.
  $\longrightarrow$ Observed also by **JLAB**: **Tedeschi et al.** and **B. Dey** dissertation.
- **Conventional model of Pomeron plus π and η exchanges** usually can only give rise to a **monotonically-increasing** behavior.
- We would like to see whether this **local peak** can be explained as a **resonance**.
- In order to **check** this assumption, we apply the results on $\gamma p \to \phi p$ to $\gamma d \to \phi p n$ to see if we can **describe the latter**.

Reaction model for $\gamma p \to \phi p$

- Here are the **tree-level diagrams** calculated in our model in an **effective Lagrangian** approach.

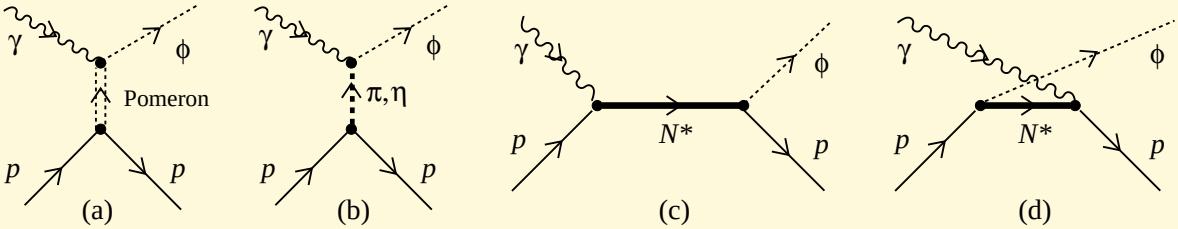

N^* is the postulated resonance.

- p_i is the 4-momentum of the **proton** in the **initial** state,
- k is the 4-momentum of the **photon** in the **initial** state,
- p_f is the 4-momentum of the **proton** in the **final** state,
- q is the 4-momentum of the ϕ in the **final** state.

Pomeron exchange

We follow the work of **Donnachie, Landshoff, and Nachtmann**

$$i\mathcal{M} = i\bar{u}_f(p_f)\epsilon_\phi^{*\mu} M_{\mu\nu} u_i(p_i)\epsilon_\gamma^\nu$$

$$M_{\mu\nu} = M(s,t)\Gamma_{\mu\nu}$$

$$M(s,t) = C_P F_1(t) F_2(t) \frac{1}{s}\left(\frac{s - s_{th}}{4}\right)^{\alpha_P(t)} \exp\left[-i\pi\alpha_P(t)/2\right]$$

- $\Gamma^{\mu\nu}$ is chosen to maintain **gauge invariance**.
- The **strength factor** $C_P = 3.65$ is chosen to **fit** the **total cross sections** data at **high energy**.
- The **threshold factor** $s_{th} = 1.3$ **GeV**^{2} is chosen to **match** the **forward differential cross sections** data at around $E_\gamma = 6$ **GeV**.

π and η exchanges

- For **t-channel exchange involving π and η**, we use

$$\begin{aligned}\mathcal{L}_{\gamma\phi M} &= \frac{e g_{\gamma\phi M}}{m_\phi}\epsilon^{\mu\nu\alpha\beta}\partial_\mu\phi_\nu\partial_\alpha A_\beta\varphi_M \\ \mathcal{L}_{MNN} &= \frac{g_{MNN}}{2M_N}\bar{\psi}\gamma^\mu\gamma^5\psi\partial_\mu\varphi_M\end{aligned}$$

  with $M = (\pi, \eta)$.

- We choose $g_{\pi NN} = 13.26$, $g_{\eta NN} = 1.12$, $g_{\gamma\phi\pi} = -0.14$, and $g_{\gamma\phi\eta} = -0.71$.

- Form factor at **each vertex** in the t-channel diagram is

$$F_{MNN}(t) = F_{\gamma\phi M}(t) = \frac{\Lambda_M^2 - m_M^2}{\Lambda_M^2 - t}$$

- The value $\Lambda_M = 1.2$ **GeV** is taken for **both** $M = (\pi, \eta)$.

Resonances

- Only **spin** $1/2$ or $3/2$ because the **resonance is close to the threshold**.
- **Lagrangian densities** that couple **spin-**$1/2$ and $3/2$ particles to γN or ϕN channels are

$$\begin{aligned}
\mathcal{L}^{1/2^\pm}_{\phi NN^*} &= g^{(1)}_{\phi NN^*}\bar{\psi}_N\Gamma^\pm\gamma^\mu\psi_{N^*}\phi_\mu + g^{(2)}_{\phi NN^*}\bar{\psi}_N\Gamma^\pm\sigma_{\mu\nu}G^{\mu\nu}\psi_{N^*}, \\
\mathcal{L}^{3/2^\pm}_{\phi NN^*} &= ig^{(1)}_{\phi NN^*}\bar{\psi}_N\Gamma^\pm\left(\partial^\mu\psi^\nu_{N^*}\right)\tilde{G}_{\mu\nu} + g^{(2)}_{\phi NN^*}\bar{\psi}_N\Gamma^\pm\gamma^5\left(\partial^\mu\psi^\nu_{N^*}\right)G_{\mu\nu} \\
&+ ig^{(3)}_{\phi NN^*}\bar{\psi}_N\Gamma^\pm\gamma^5\gamma_\alpha\left(\partial^\alpha\psi^\nu_{N^*} - \partial^\nu\psi^\alpha_{N^*}\right)\left(\partial^\mu G_{\mu\nu}\right),
\end{aligned}$$

where $G_{\mu\nu} = \partial_\mu\phi_\nu - \partial_\nu\phi_\mu$ and $\tilde{G}_{\mu\nu} = \frac{1}{2}\epsilon_{\mu\nu\alpha\beta}G^{\alpha\beta}$. The operator $\Gamma^\pm$ are given by $\Gamma^+ = 1$ and $\Gamma^- = \gamma_5$, depending on the parity of the resonance N^*.

- For the γNN^* **vertices**, simply change $g_{\phi NN^*} \to eg_{\gamma NN^*}$ and $\phi_\mu \to A_\mu$.

- **Current conservation** fixes $g^{(1)}_{\gamma NN^*} \to 0$ for $J^P = 1/2^\pm$ and the term **proportional** to $g^{(3)}_{\gamma NN^*}$ **vanishes** in the case of **real photon**.
- The **effect of the width** is taken into account in a **Breit-Wigner** form by replacing the usual denominator $p^2 - M^2_{N^*} \to p^2 - M^2_{N^*} + iM_{N^*}\Gamma_{N^*}$.
- The **form factor** for the **vertices** used in the s- and u-**channel diagrams** is

$$F_{N^*}(p^2) = \frac{\Lambda^4}{\Lambda^4 + (p^2 - M^2_{N^*})^2}$$

with $\Lambda = 1.2$ **GeV** for **all resonances**.

Fitting to $\gamma p \to \phi p$ experimental data

- We include only **one resonance at a time**.
- We fit only **masses**, **widths**, and **coupling constants** of the resonances to the experimental data, while **other parameters are fixed** during fitting.
- Experimental data to fit
  - **Differential cross sections** (DCS) at **forward angle**
  - **DCS as a function of t** at eight incoming photon energy bins
  - **Nine spin-density matrix elements (SDME)** at three incoming photon energy bins

Results for $\gamma p \to \phi p$

- Both $J^P = 1/2^\pm$ resonances **cannot fit the data**.
- **DCS at forward angle and as a function of** t are markedly **improved** by the inclusion of the $J^P = 3/2^\pm$ resonances.
- In general, **SDME are also improved** by both $J^P = 3/2^\pm$ resonances.
- **Decay angular distributions**, not used in the fitting procedure, can also be explained well.
- We study the effect of the resonance to the **DCS of** $\gamma p \to \omega p$.
  $\longrightarrow$ The resonance seems to have a **considerable amount of strangeness content**.

DCS of $\gamma p \to \phi p$ at forward angle

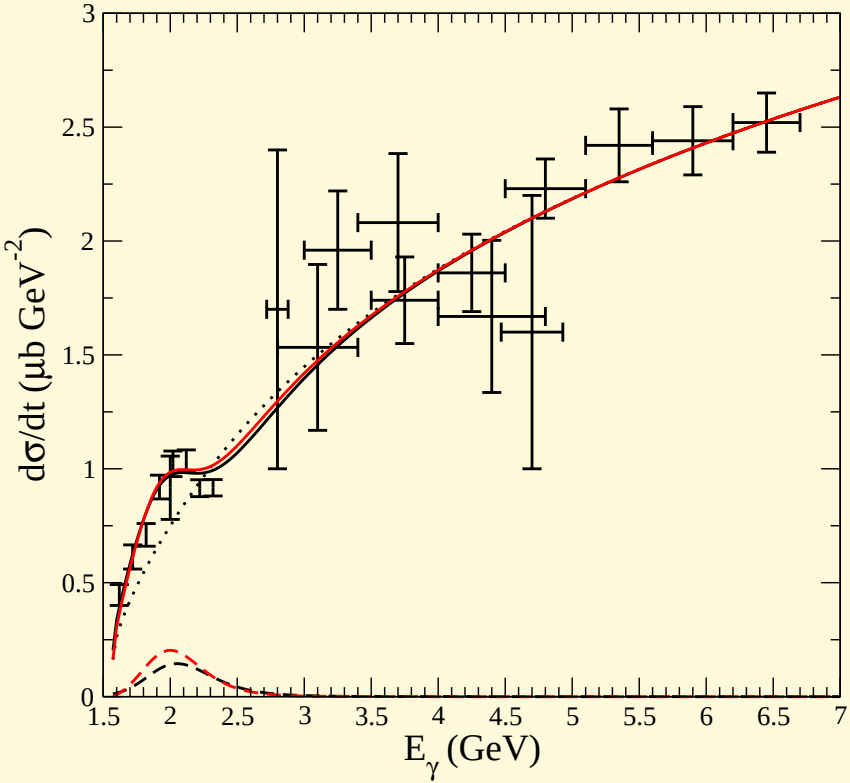

Black$\to J^P = 3/2^-$ **Red**$\to$ $J^P = 3/2^+$

Total $\to$ full, Nonresonant $\to$ dotted, Resonant $\to$ dashed

DCS of $\gamma p \to \phi p$ as a function of t

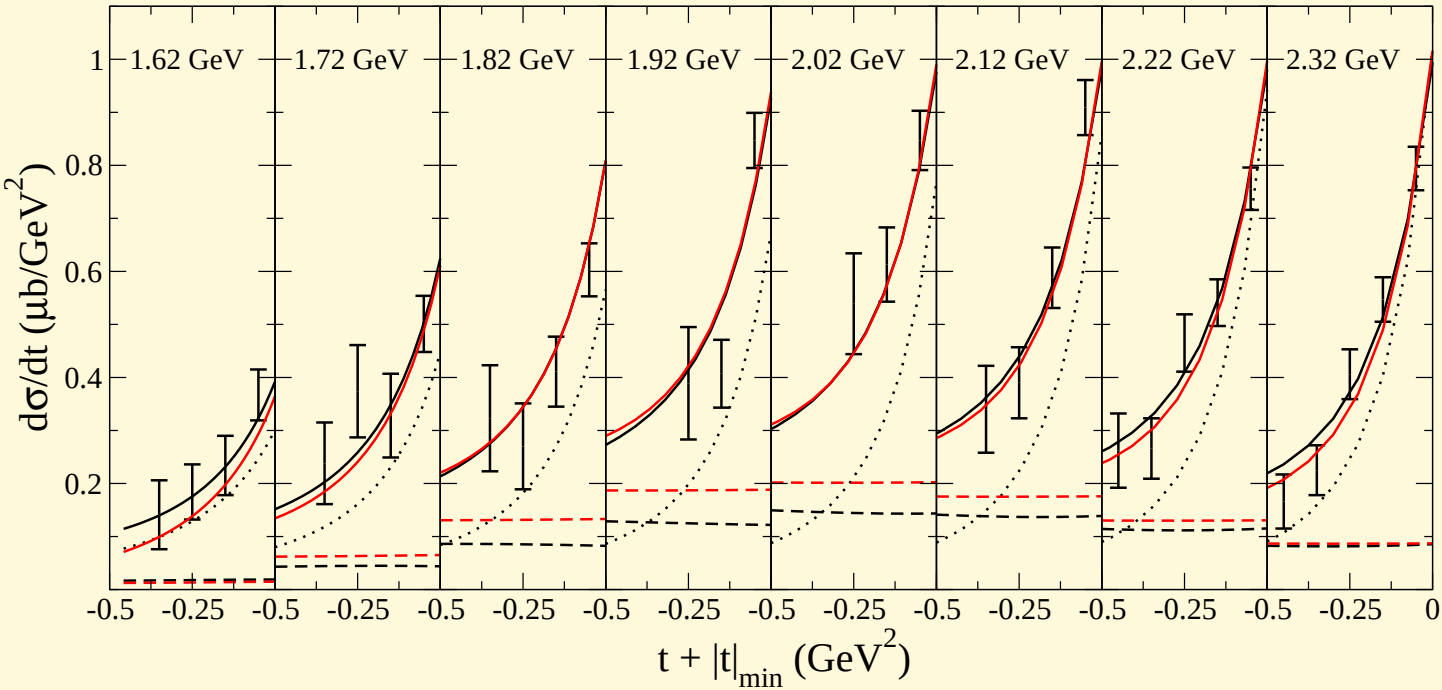

Black$\to J^P = 3/2^-$ **Red**$\to$ $J^P = 3/2^+$

Total $\to$ full, Nonresonant $\to$ dotted, Resonant $\to$ dashed

SDME of $\gamma p \to \phi p$ as a function of t

$1.77 < E_\gamma < 1.97$ GeV

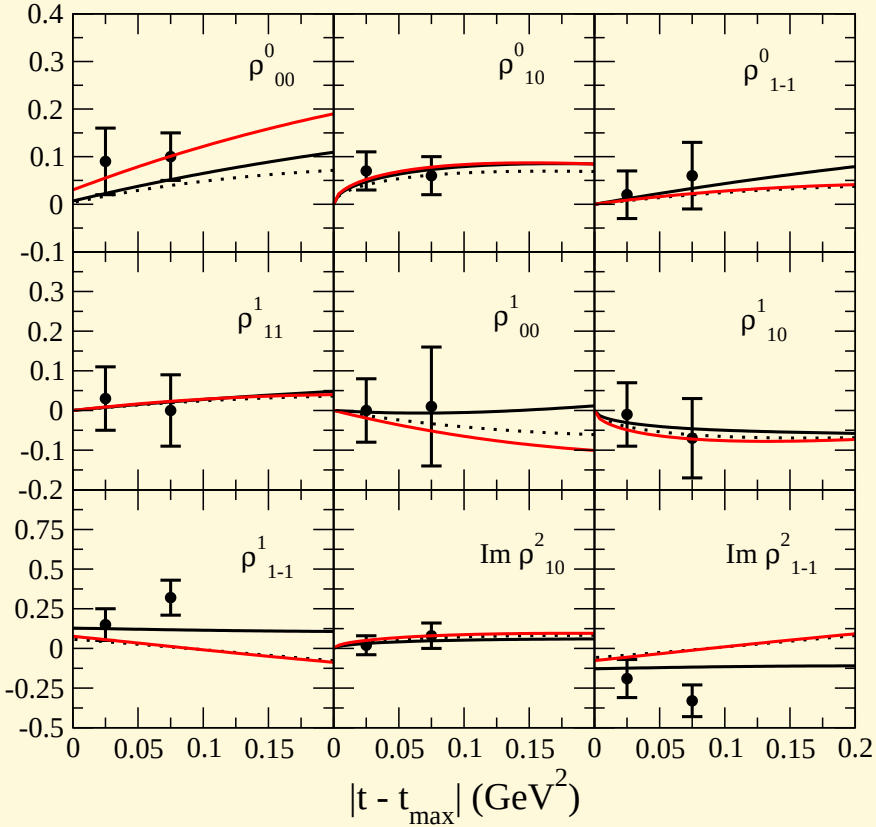

SDME of $\gamma p \to \phi p$ as a function of t

$1.97 < E_\gamma < 2.17$ GeV

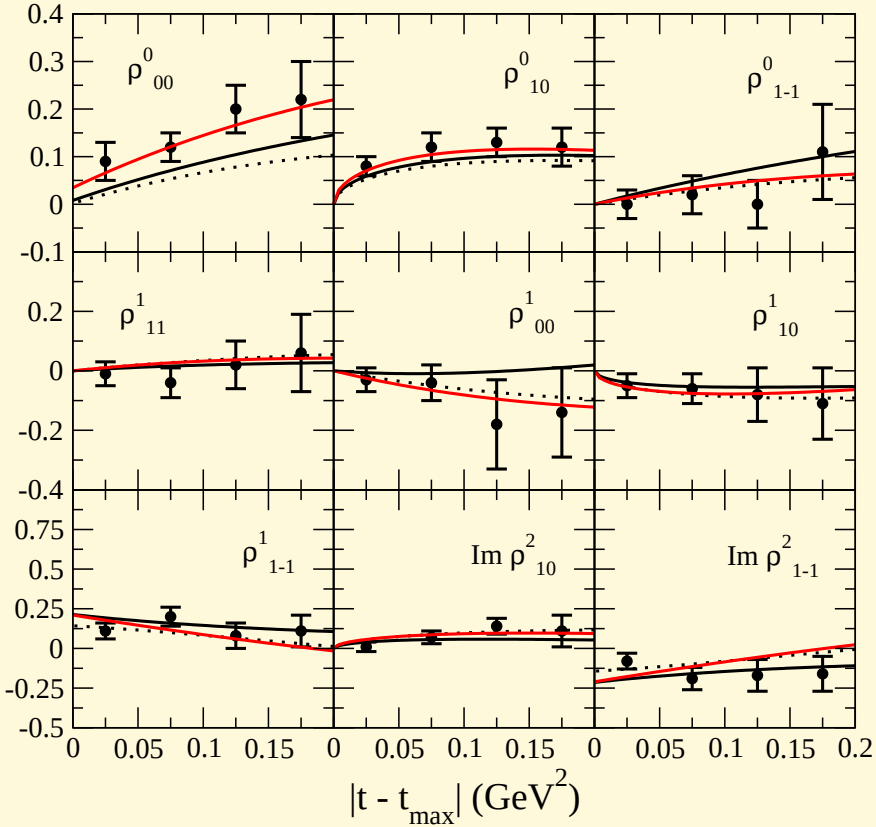

SDME of $\gamma p \to \phi p$ as a function of t

$2.17 < E_\gamma < 2.37$ GeV

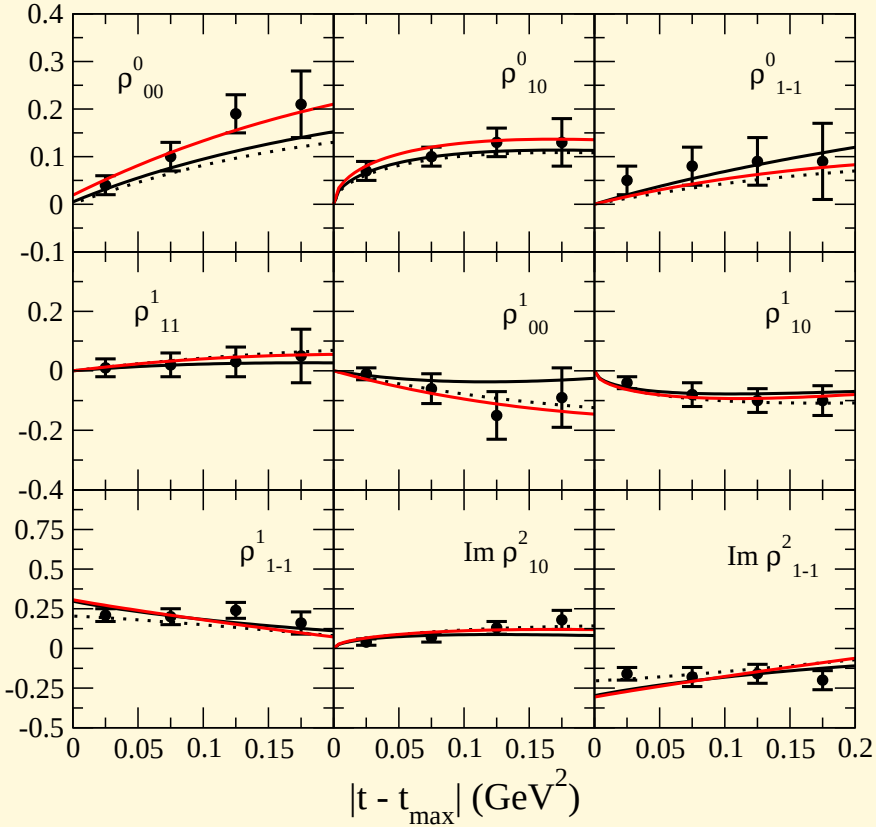

Decay angular distributions at two energy bins [$E_\gamma = 2.07$ GeV (upper) and $E_\gamma = 2.27$ GeV (lower)]

Not fitted

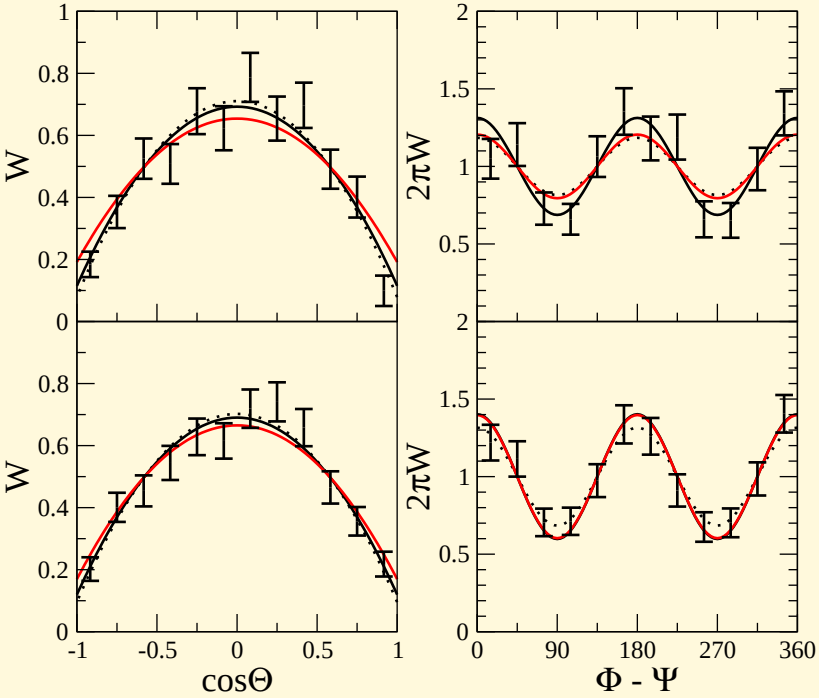

Decay angular distributions at two energy bins [$E_\gamma = 2.07$ GeV (upper) and $E_\gamma = 2.27$ GeV (lower)]

Not fitted

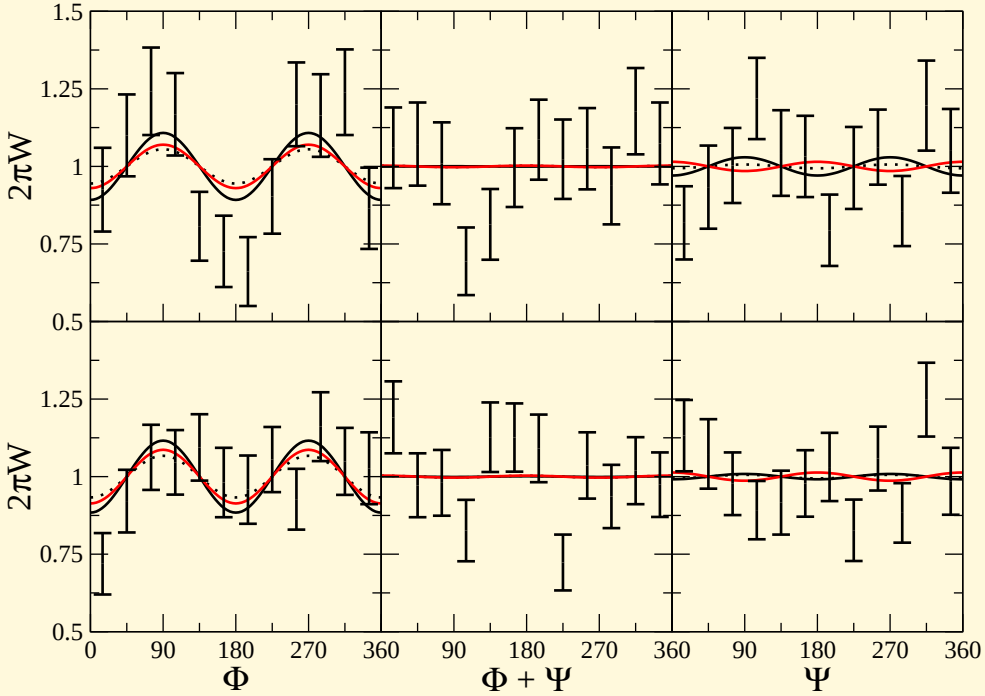

(c)

	$J^P = 3/2^+$	$J^P = 3/2^-$
M_{N^*}(GeV)	**2.08 ± 0.04**	**2.08 ± 0.04**
Γ_{N^*}(GeV)	**0.501 ± 0.117**	**0.570 ± 0.159**
$eg^{(1)}_{\gamma NN^*} g^{(1)}_{\phi NN^*}$	0.003 ± 0.009	−0.205 ± 0.083
$eg^{(1)}_{\gamma NN^*} g^{(2)}_{\phi NN^*}$	−0.084 ± 0.057	−0.025 ± 0.017
$eg^{(1)}_{\gamma NN^*} g^{(3)}_{\phi NN^*}$	0.025 ± 0.076	−0.033 ± 0.017
$eg^{(2)}_{\gamma NN^*} g^{(1)}_{\phi NN^*}$	0.002 ± 0.006	−0.266 ± 0.127
$eg^{(2)}_{\gamma NN^*} g^{(2)}_{\phi NN^*}$	−0.048 ± 0.047	−0.033 ± 0.032
$eg^{(2)}_{\gamma NN^*} g^{(3)}_{\phi NN^*}$	0.014 ± 0.040	−0.043 ± 0.032
χ^2/N	0.891	0.821

- The ratio $A_{1/2}/A_{3/2} = 1.05$ for the $J^P = 3/2^-$ resonance.
  $\longrightarrow$ Similarity to $D_{13}(2120)$ is interesting to note.
  (PDG lists $A_{1/2}/A_{3/2} = 0.83$)
- The ratio $A_{1/2}/A_{3/2} = 0.89$ for the $J^P = 3/2^+$ resonance.

Predictions for single polarization observables for $\gamma p \to \phi p$

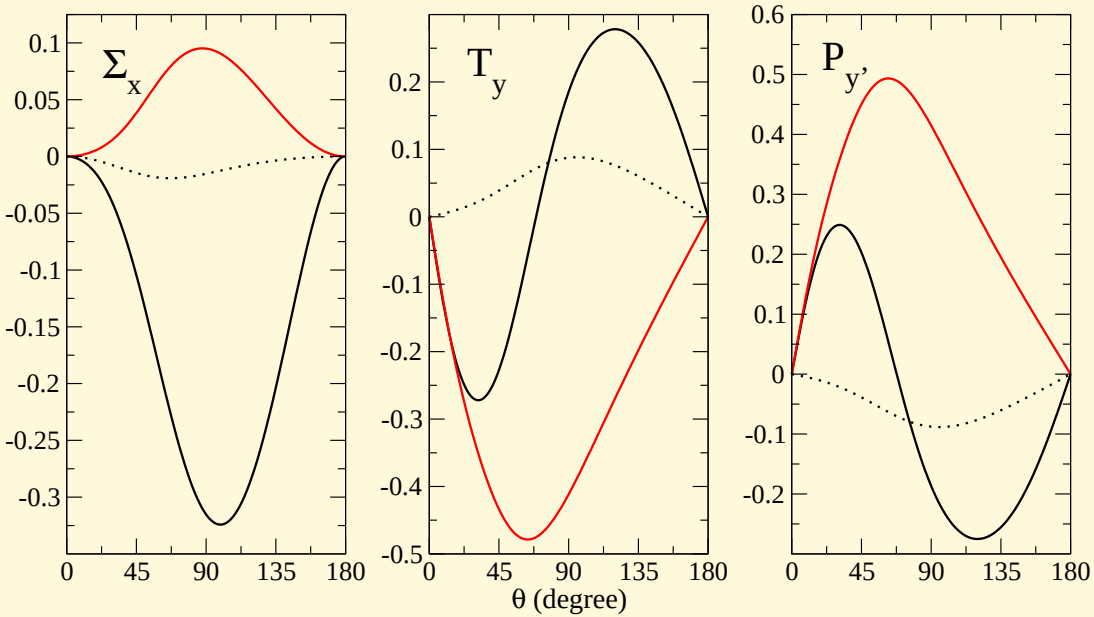

Asymmetries of the **polarized beam** Σ_x, **polarized target** T_y, and **recoil polarization** $P_{y'}$

Predictions for double polarization observables for $\gamma p \to \phi p$

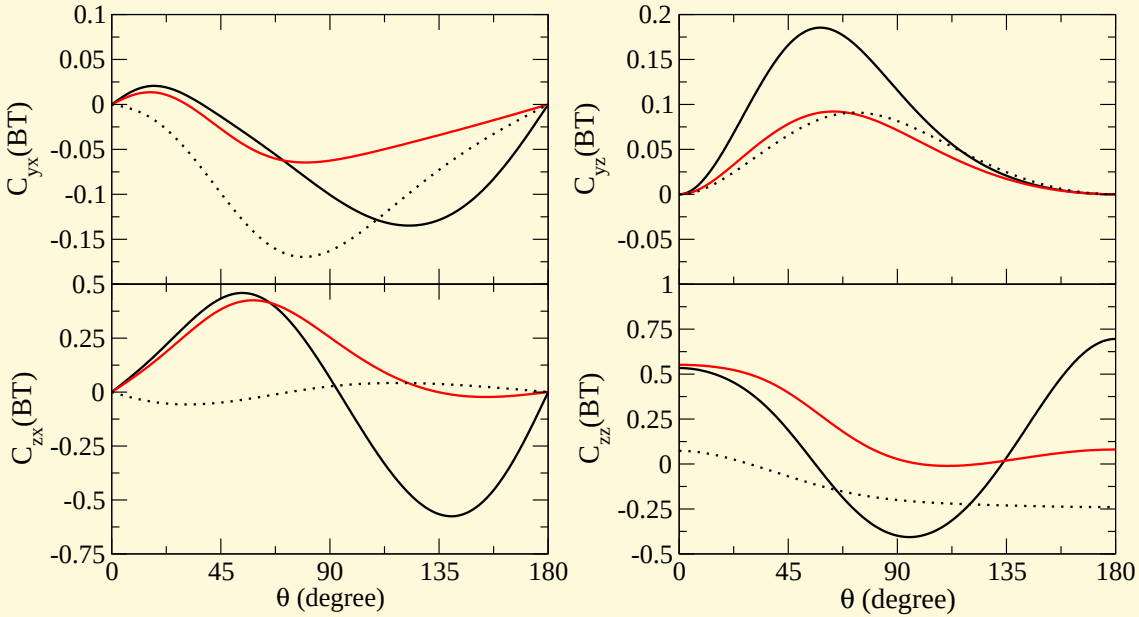

Beam-target (BT) asymmetries C_{yx}^{BT}, C_{yz}^{BT}, C_{zx}^{BT}, and C_{zz}^{BT}, with the **photon beam and the nucleon target polarized**

Reaction model for $\gamma d \to \phi pn$

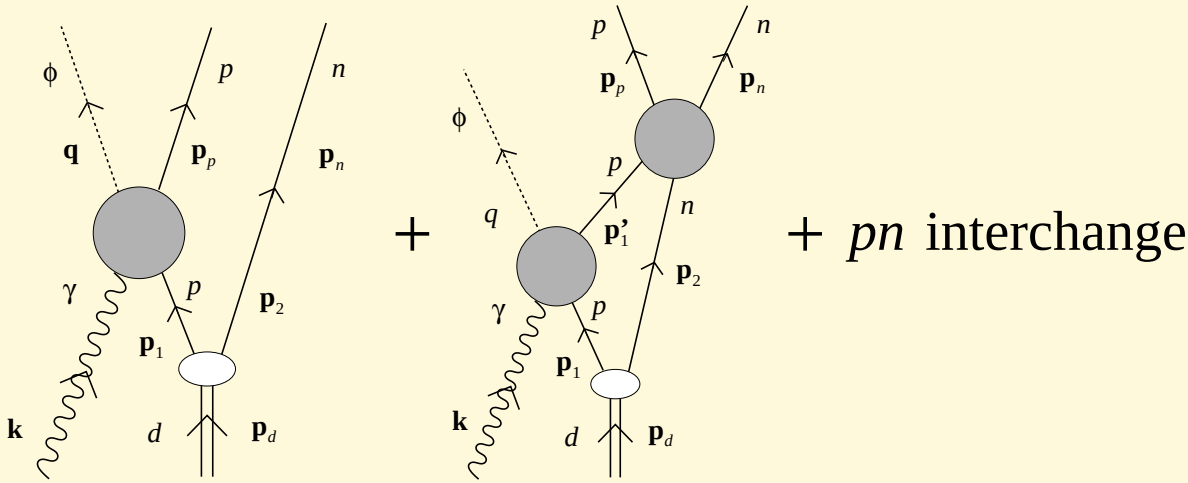

- **Fermi motion** of the proton and neutron inside the deuteron is included using **deuteron wave function** calculated by **Machleidt** in PRC **63** 024001 (2001).
- **Final-state interactions (FSI) of** pn is included using **GWU-SAID phase-shift data** on pn scattering.

- The **same model** for the amplitude of $\gamma p \to \phi p$.
- A $J^P = 3/2^-$ **resonance** is also present in the $\gamma n \to \phi n$ amplitude
  - **For $\phi n n^*$ vertex**, ϕp and ϕn cases are **the same since ϕ is an $I = 0$ particle**.
  - **For $\gamma n n^*$ vertex**, we assume that the **resonance** would have the **same properties as a CQM state with the same J^P and similar value of $A_{1/2}/A_{3/2}$ for the γp decay**
    $\longrightarrow N\frac{3}{2}^-(2095)[D_{13}]_5$ in **Capstick's work** in PRD **46**, 2864 (1992), the **only one with positive value of $A_{1/2}/A_{3/2}$ for γp in the energy region**.
- $J^P = 3/2^+$ **resonance** has not been calculated yet.

Results for $\gamma d \to \phi pn$

- Notice that **no fitting is performed** to the LEPS data on DCS [PLB **684** 6-10 (2010)] and SDME [PRC **82** 015205 (2010)] of $\gamma d \to \phi pn$ from **Chang et al.**.
- We found a **very good agreement** with the LEPS experimental data on both observables.
- Notice that **LEPS DCS data** given with **error bars** are actually processed **to remove the effect of Fermi motion**.
- **Our reconstructed data**, given in **grey bands**, **reinstate the removed Fermi motion**.
  $\longrightarrow$ We actually **discussed** this reconstruction with **Chang** from the **LEPS Collaboration**.
- Both **resonance** and pn **FSI** effects are found to be **large**.
  $\longrightarrow$ **Without them**, the DCS data **cannot** be described.

DCS of $\gamma d \to \phi pn$
Not fitted

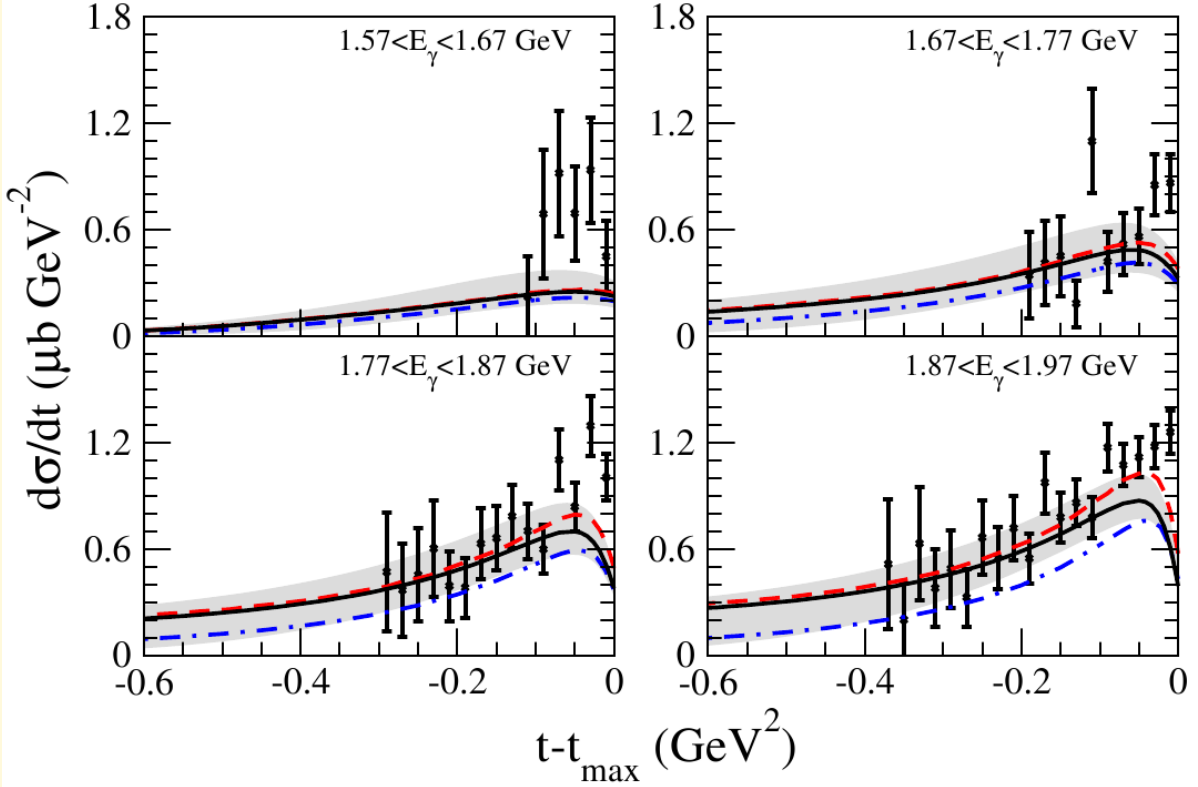

Blue → no resonance, no pn FSI; **Red** → resonance, no pn FSI; **Black** → resonance, pn FSI; **Grey bands** → reconstructed data

DCS of $\gamma d \to \phi pn$
Not fitted

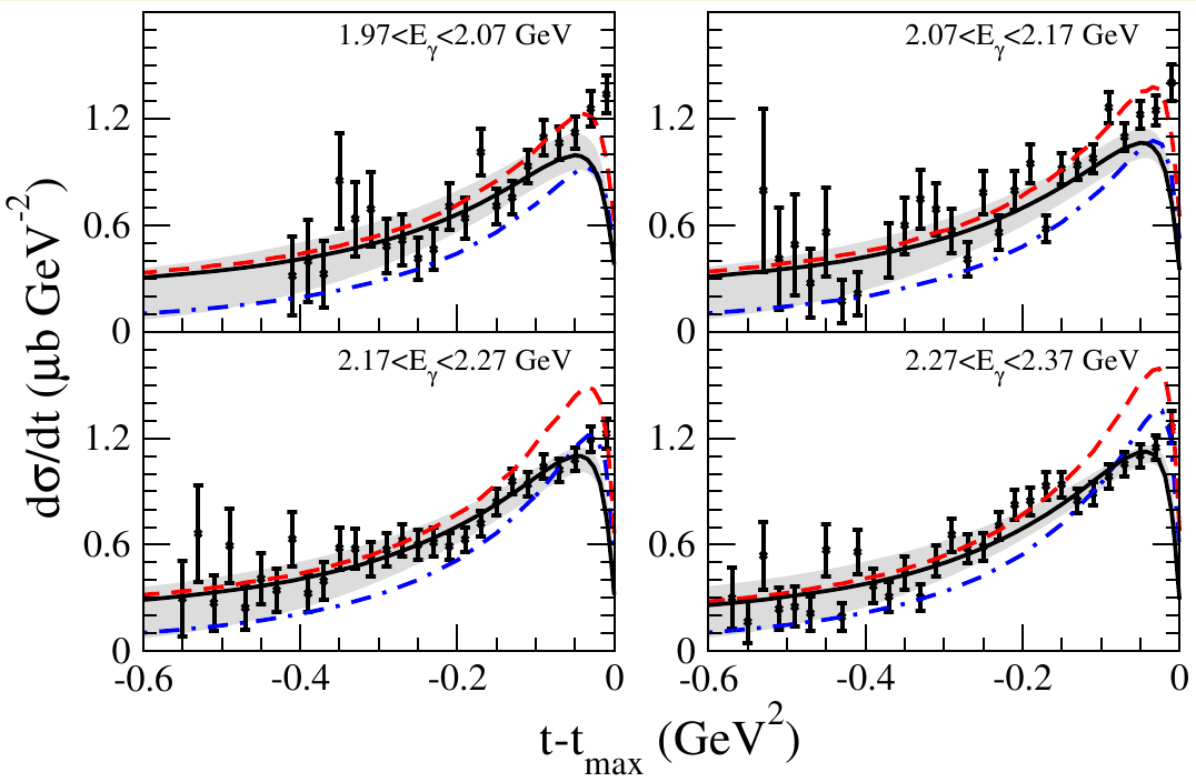

SDME of $\gamma d \to \phi pn$ as a function of t

Not fitted

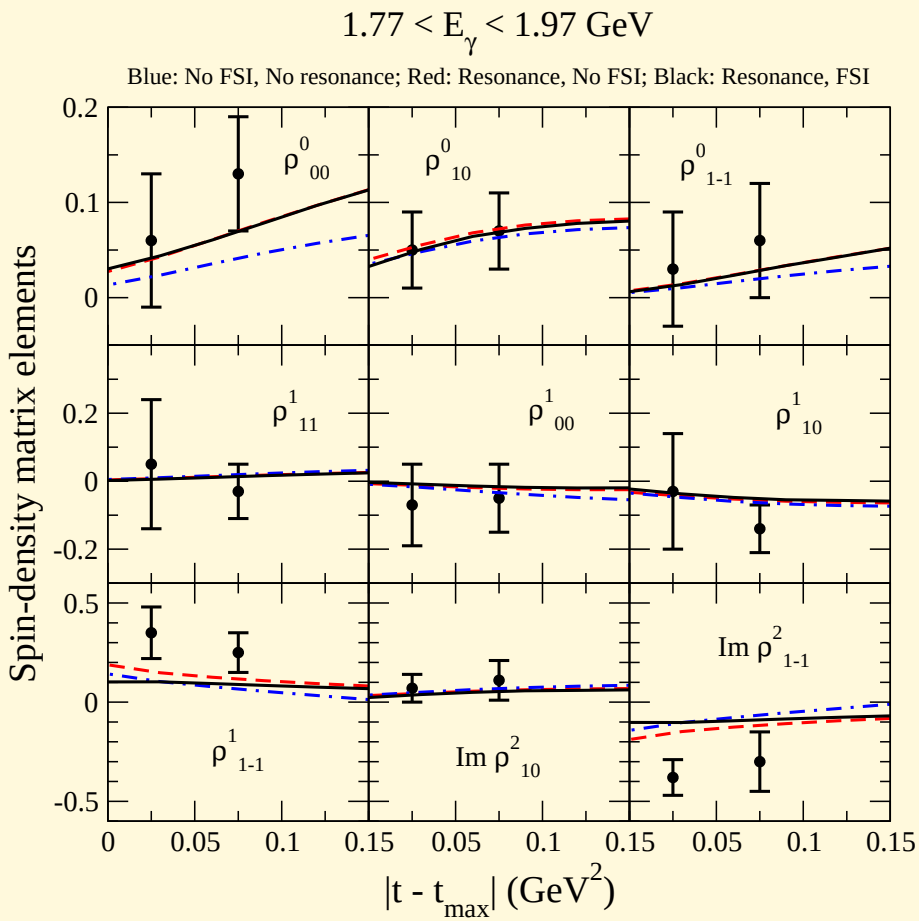

SDME of $\gamma d \to \phi pn$ as a function of t
Not fitted

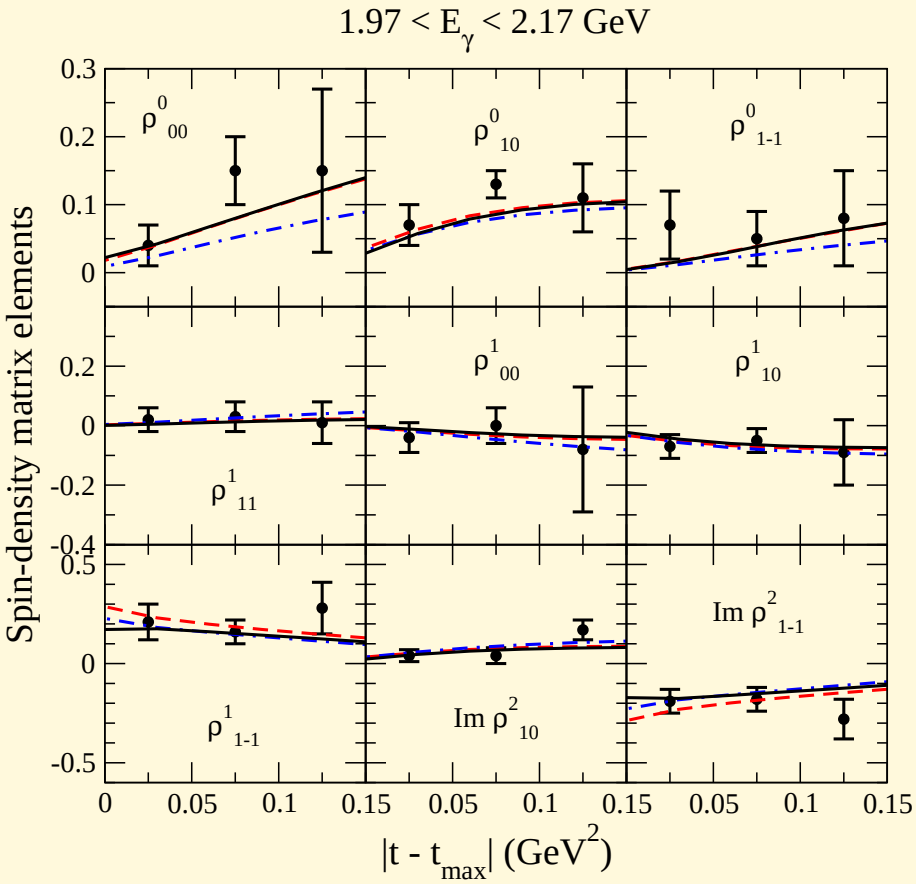

SDME of $\gamma d \to \phi pn$ as a function of t
Not fitted

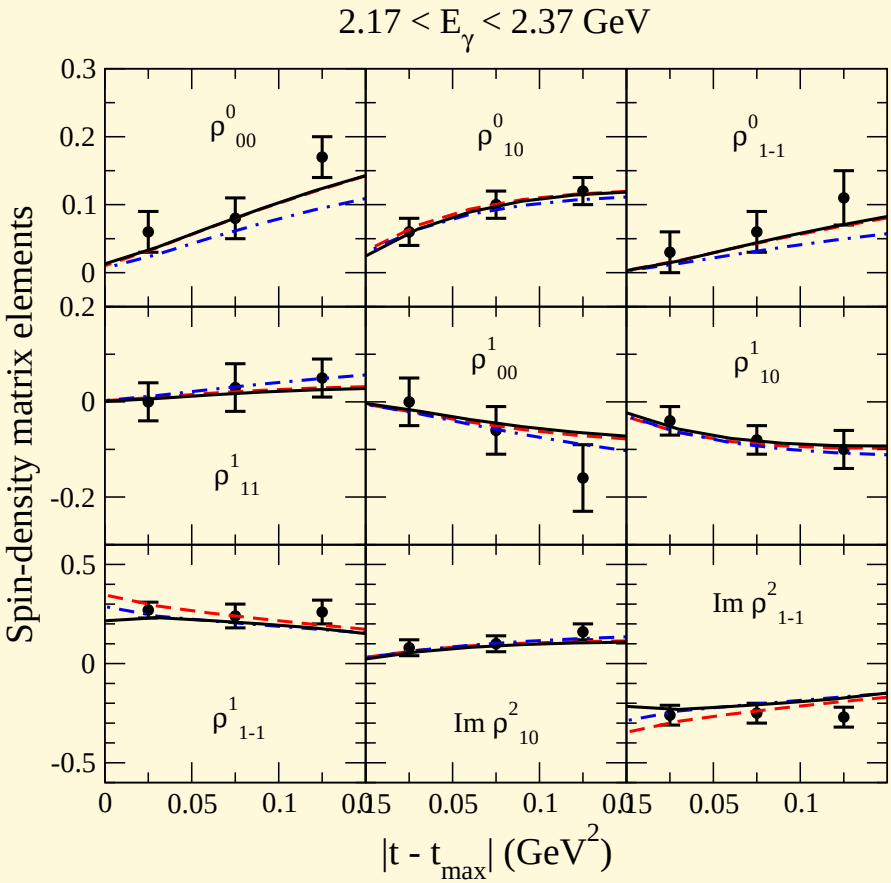

Summary and conclusions

- **Inclusion of a resonance is needed** to explain the **non-monotonic behavior** in the DCS $\gamma p \to \phi p$ near threshold.
- Resonance with $J = 3/2$ of either parity is preferred for $\gamma p \to \phi p$, while $J^P = 1/2^{\pm}$ cannot fit the data.
- We can also explain the experimental data on the DCS and SDME of $\gamma d \to \phi pn$ very well using $J^P = 3/2^-$ resonance.
  $\longrightarrow$ **Final-state interaction of** pn and **resonance effects** are found to be **large** and **important** to describe the data.
- **Similarity between the** $J^P = 3/2^-$ **and** $D_{13}(2120)$ is interesting to note.
  $\longrightarrow$**Rather similar value of the ratio of helicity amplitudes** $A_{1/2}/A_{3/2}$ **for** γp **(Ours = 1.05, PDG = 0.83)**.
- The resonance seems to have a **considerable amount of strangeness content**.
  $\longrightarrow$ Based on a **separate study** on its effect on $\gamma p \to \omega p$.

Outlooks

- We plan to work out $\gamma d \to \phi d$ for even **more consistent** check.
- **Coupled-channel analysis for ϕN, $K\Sigma$, and $K\Lambda$** will also be interesting to do.
  $\longrightarrow$ JLAB already has the data.
- More experiments, e.g. measurement of **single and double polarizations**, would be helpful to check our predictions.
  $\longrightarrow$ **Asymmetry of the polarized beam Σ_x** would be **ideal** to distinguish the parity since **different parities** have **different signs**.

THANK YOU!

Pomeron exchange

We follow the work of **Donnachie, Landshoff, and Nachtmann**

$$i\mathcal{M} = i\bar{u}_f(p_f)\epsilon_\phi^{*\mu} M_{\mu\nu} u_i(p_i)\epsilon_\gamma^\nu$$

$$M_{\mu\nu} = \Gamma_{\mu\nu} M(s,t)$$

with

$$\begin{aligned}\Gamma_{\mu\nu} &= \not{k}\left(g_{\mu\nu} - \frac{q_\mu q_\nu}{q^2}\right) - \gamma_\nu\left(k_\mu - q_\mu\frac{k\cdot q}{q^2}\right) \\ &- \left(q_\nu - \bar{p}_\nu\frac{k\cdot q}{p\cdot k}\right)\left(\gamma_\mu - \not{q}\frac{q_\mu}{q^2}\right) \quad ; \quad \bar{p} = \frac{1}{2}(p_f + p_i)\end{aligned}$$

where $\Gamma^{\mu\nu}$ is chosen to maintain **gauge invariance**, and

A1

$$M(s,t) = C_P F_1(t) F_2(t) \frac{1}{s} \left(\frac{s - s_{th}}{4} \right)^{\alpha_P(t)} \exp\left[-i\pi\alpha_P(t)/2\right]$$

in which

$$\begin{aligned} F_1(t) &= \frac{4m_N^2 - 2.8t}{(4m_N^2 - t)(1 - t/0.7)^2} \\ F_2(t) &= \frac{2\mu_0^2}{(1 - t/M_\phi^2)(2\mu_0^2 + M_\phi^2 - t)}; \quad \mu_0^2 = 1.1 \text{ GeV}^2 \end{aligned}$$

$F_1(t) \rightarrow$ **isoscalar EM form-factor of the nucleon**
$F_2(t) \rightarrow$ **form-factor for the ϕ-γ-Pomeron coupling**
Pomeron trajectory $\alpha_P = 1.08 + 0.25t$.

- The **strength factor** $C_P = 3.65$ is chosen to **fit** the **total cross sections** data at **high energy**.
- The **threshold factor** $s_{th} = 1.3$ **GeV**^{2} is chosen to **match** the **forward differential cross sections** data at around $E_\gamma = 6$ **GeV**.

A2

Effects on $\gamma p \to \omega p$

- From the $\phi - \omega$ **mixing**, we expect the resonance to also contribute to ω **photoproduction**.
- The coupling constants $g_{\phi NN^*}$ and $g_{\omega NN^*}$ are **related**, and in our study we choose to use the so-called **"minimal" parametrization**,

$$g_{\phi NN^*} = -\mathbf{x}_{\mathrm{OZI}} \tan\Delta\theta_V g_{\omega NN^*}$$

  where $\mathbf{x}_{\mathrm{OZI}} = \mathbf{1}$ is the **ordinary $\phi - \omega$ mixing**.
- By using $x_{\mathbf{OZI}} = 12$ for the $J^P = 3/2^-$ resonance and $x_{\mathbf{OZI}} = 9$ for the $J^P = 3/2^+$ resonance, we found that we can **explain quite well** the **DCS of ω photoproduction**.
- The **large value of $x_{\mathbf{OZI}}$** indicates that the resonance has a **considerable amount of strangeness content**.

B1

DCS of $\gamma p \to \omega p$ as a function of t

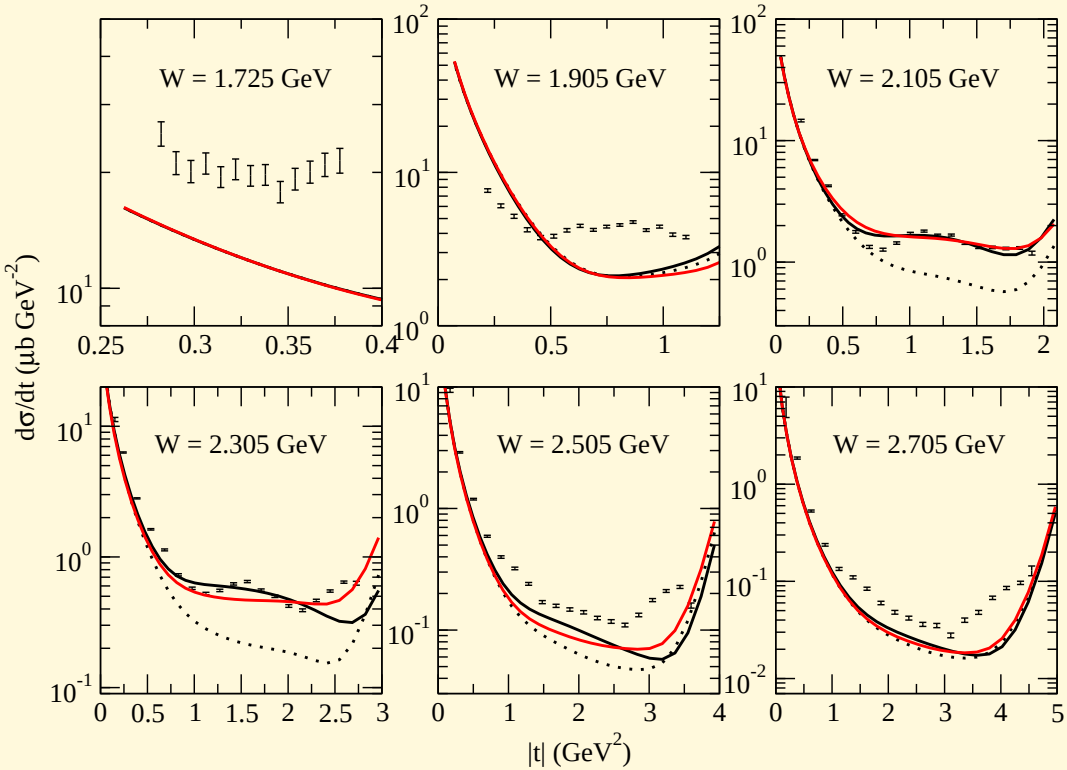

Data from M. Williams, PRC 80, 065209 (2009)

B2